

# Elliptic flow of $\Lambda$ hyperons in Pb+Pb collisions at 158A GeV

C. Alt,<sup>9</sup> T. Anticic,<sup>21</sup> B. Baatar,<sup>8</sup> D. Barna,<sup>4</sup> J. Bartke,<sup>6</sup> L. Betev,<sup>10</sup> H. Bialkowska,<sup>19</sup> C. Blume,<sup>9</sup> B. Boimska,<sup>19</sup> M. Botje,<sup>1</sup> J. Bracinić,<sup>3</sup> R. Bramm,<sup>9</sup> P. Bunčić,<sup>10</sup> V. Cerny,<sup>3</sup> P. Christakoglou,<sup>2</sup> P. Chung,<sup>23</sup> O. Chvala,<sup>15</sup> J.G. Cramer,<sup>17</sup> P. Csató,<sup>4</sup> P. Dinkelaker,<sup>9</sup> V. Eckardt,<sup>14</sup> D. Flierl,<sup>9</sup> Z. Fodor,<sup>4</sup> P. Foka,<sup>7</sup> V. Friese,<sup>7</sup> J. Gál,<sup>4</sup> M. Gaździcki,<sup>9,12</sup> G. Georgopoulos,<sup>2</sup> E. Gładysz,<sup>6</sup> K. Grebieszko,<sup>22</sup> S. Hegyi,<sup>4</sup> C. Höhne,<sup>13</sup> K. Kadija,<sup>21</sup> A. Karev,<sup>14</sup> M. Kliemant,<sup>9</sup> S. Kniege,<sup>9</sup> V.I. Kolesnikov,<sup>8</sup> E. Kornas,<sup>6</sup> R. Korus,<sup>12</sup> M. Kowalski,<sup>6</sup> I. Kraus,<sup>7</sup> M. Kreps,<sup>3</sup> R. Lacey,<sup>23</sup> A. Laszlo,<sup>4</sup> M. van Leeuwen,<sup>1</sup> P. Lévai,<sup>4</sup> L. Litov,<sup>18</sup> B. Lungwitz,<sup>9</sup> M. Makariev,<sup>18</sup> A.I. Malakhov,<sup>8</sup> M. Mateev,<sup>18</sup> G.L. Melkumov,<sup>8</sup> A. Mischke,<sup>7</sup> M. Mitrovski,<sup>9</sup> J. Molnár,<sup>4</sup> St. Mrówczyński,<sup>12</sup> V. Nikolic,<sup>21</sup> G. Pála,<sup>4</sup> A.D. Panagiotou,<sup>2</sup> D. Panayotov,<sup>18</sup> A. Petridis,<sup>2</sup> M. Pikna,<sup>3</sup> D. Prindle,<sup>17</sup> F. Pühlhofer,<sup>13</sup> R. Renfordt,<sup>9</sup> C. Roland,<sup>5</sup> G. Roland,<sup>5</sup> M. Rybczyński,<sup>12</sup> A. Rybicki,<sup>6</sup> A. Sandoval,<sup>7</sup> N. Schmitz,<sup>14</sup> T. Schuster,<sup>9</sup> P. Seyboth,<sup>14</sup> F. Siklér,<sup>4</sup> B. Sitar,<sup>3</sup> E. Skrzypczak,<sup>20</sup> G. Stefanek,<sup>12,\*</sup> R. Stock,<sup>9</sup> C. Strabel,<sup>9</sup> H. Ströbele,<sup>9</sup> T. Susa,<sup>21</sup> I. Szentpétery,<sup>4</sup> J. Sziklai,<sup>4</sup> P. Szymanski,<sup>10,19</sup> V. Trubnikov,<sup>19</sup> D. Varga,<sup>4,10</sup> M. Vassiliou,<sup>2</sup> G.I. Veres,<sup>4,5</sup> G. Vesztergombi,<sup>4</sup> D. Vranić,<sup>7</sup> A. Wetzler,<sup>9</sup> Z. Włodarczyk,<sup>12</sup> A. Wojtaszek,<sup>12</sup> I.K. Yoo,<sup>16</sup> and J. Zimányi<sup>4,†</sup>

(The NA49 collaboration)

<sup>1</sup>NIKHEF, Amsterdam, Netherlands.

<sup>2</sup>Department of Physics, University of Athens, Athens, Greece.

<sup>3</sup>Comenius University, Bratislava, Slovakia.

<sup>4</sup>KFKI Research Institute for Particle and Nuclear Physics, Budapest, Hungary.

<sup>5</sup>MIT, Cambridge, USA.

<sup>6</sup>The H.Niewodniczanski Institute of Nuclear Physics, Polish Academy of Sciences, Cracow, Poland.

<sup>7</sup>Gesellschaft für Schwerionenforschung (GSI), Darmstadt, Germany.

<sup>8</sup>Joint Institute for Nuclear Research, Dubna, Russia.

<sup>9</sup>Fachbereich Physik der Universität, Frankfurt, Germany.

<sup>10</sup>CERN, Geneva, Switzerland.

<sup>11</sup>University of Houston, Houston, TX, USA.

<sup>12</sup>Institute of Physics Świętokrzyska Academy, Kielce, Poland.

<sup>13</sup>Fachbereich Physik der Universität, Marburg, Germany.

<sup>14</sup>Max-Planck-Institut für Physik, Munich, Germany.

<sup>15</sup>Institute of Particle and Nuclear Physics, Charles University, Prague, Czech Republic.

<sup>16</sup>Department of Physics, Pusan National University, Pusan, Republic of Korea.

<sup>17</sup>Nuclear Physics Laboratory, University of Washington, Seattle, WA, USA.

<sup>18</sup>Atomic Physics Department, Sofia University St. Kliment Ohridski, Sofia, Bulgaria.

<sup>19</sup>Institute for Nuclear Studies, Warsaw, Poland.

<sup>20</sup>Institute for Experimental Physics, University of Warsaw, Warsaw, Poland.

<sup>21</sup>Rudjer Boskovic Institute, Zagreb, Croatia.

<sup>22</sup>Warsaw University of Technology, Warsaw, Poland.

<sup>23</sup>Department of Chemistry, SUNY Stony Brook, USA.

The elliptic flow of  $\Lambda$  hyperons has been measured by the NA49 collaboration at the CERN-SPS in semi-central Pb+Pb collisions at 158A GeV. The standard method of correlating particles with the event plane was used. Measurements of  $v_2$  near mid-rapidity are reported as a function of rapidity, centrality and transverse momentum. Elliptic flow of  $\Lambda$  particles increases both with the impact parameter and with the transverse momentum. It is compared with  $v_2$  for pions and protons as well as with model calculations. The observation of significant elliptic flow and its mass dependence suggest strong collective behavior of the matter produced in collisions of heavy nuclei already at the SPS. Scaling properties of elliptic flow of different particle species have been tested at 158A GeV. The limited  $p_T$  range of the data does not allow for a decisive test of the coalescence model.

PACS numbers: 25.75.Ld

## I. INTRODUCTION

Elliptic flow in relativistic nuclear interactions has its origin in the spatial anisotropy of the initial reaction volume in non-central collisions and in particle rescatterings in the evolving system which convert the spatial anisotropy into a momentum anisotropy [1]. The spatial

\*Corresponding author. E-mail address: stefanek@pu.kielce.pl

†Deceased

anisotropy decreases rapidly because of the fast expansion of the system [2] making the momentum anisotropy measured at the end of this evolution strongly dependent on the matter properties and the equation of state (EoS) at the early stage [3, 4]. Comparison of measured anisotropies with hydrodynamic model calculations provide an important test of the degree of thermalisation in the produced particle system at the early stage. Flow of heavy particles is affected more strongly by changes in the EoS than flow of pions [4, 5, 6].

The anisotropic flow parameters measured to date at SPS and lower energies are mainly those of pions and protons [7, 8]. RHIC experiments have measured elliptic flow for many particle species [9], including hyperons [9, 10]. In these experiments, the rapid rise of elliptic flow with transverse momentum ( $p_T$ ) up to 1.5 GeV/ $c$  and its particle-mass dependence are well reproduced by hydrodynamic models [9]. At higher values of  $p_T$  quark number scaling of elliptic flow has been observed at RHIC [10, 11] which indicates that the quark coalescence mechanism dominates hadron production in the intermediate  $p_T$  region [12]. In order to test the validity of this scenario at SPS energies we have extended elliptic flow measurements in 158A GeV Pb+Pb ( $\sqrt{s_{NN}} = 17.2$  GeV) collisions to  $\Lambda$  hyperons. In this paper, results on  $\Lambda$  elliptic flow as a function of the center of mass rapidity ( $y$ ) and transverse momentum will be presented and compared to model calculations.

## II. ANALYSIS

The main components of the NA49 detector [13] are four large-volume Time Projection Chambers (TPCs) for tracking and particle identification by energy loss ( $dE/dx$ ) measurement with a resolution of 3–6%. The TPC system consists of two vertex chambers inside the spectrometer magnets and two main chambers placed behind the magnets at both sides of the beam. Downstream of the TPCs a veto calorimeter detects projectile spectators and is used for triggering and centrality selection. The data sample consists of  $3 \times 10^6$  semi-central Pb+Pb events after online trigger selection of the 23.5% most central collisions. The events were divided into three different centrality bins, which correspond to the first three bins used in a previous analysis (see Table 1 in [8]) and are defined by centrality ranges 0-5% (bin 1), 5-12.5% (bin 2), and 12.5-23.5% (bin 3). Many model predictions are published for impact parameter ranges similar to those of our centrality classes, which are: 0-3.4 fm (bin 1), 3.4-5.3 fm (bin 2), and 5.3-7.4 fm (bin 3) for our centrality classes. The measurement in the centrality range  $\sigma/\sigma_{TOT} = 5$ –23.5% (called mid-central) is obtained by averaging the results of bins 2 plus 3 with weights corresponding to the fractions of the total cross section in these bins.

The  $\Lambda$  hyperon candidates were selected from the sample of  $V^0$ -track configurations consisting of oppositely

charged particles, which include the  $\Lambda$  decays into proton and  $\pi^-$  (branching ratio 63.9%). The identification method [14] relies on the evaluation of the invariant mass distribution and is enhanced by daughter particle identification applying a cut in  $dE/dx$  around the expectation value derived from a Bethe-Bloch parametrization. The extracted  $\Lambda$  candidates have a background contamination of 5-9% in the p- $\pi$  invariant mass window 1.108–1.124 GeV/ $c^2$ , depending on centrality. The yields of  $\Lambda$  hyperons are obtained by counting the number of entries in the invariant mass peak above the estimated background as a function of the azimuthal angle  $\phi$  of  $\Lambda$  candidates with respect to the event plane angle  $\Phi_{2EP}$ . The background is estimated from a fit of invariant mass spectra to the sum of a Lorentz distribution and a polynomial. It is subtracted in 16 bins of  $\phi - \Phi_{2EP}$ . The acceptance of  $\Lambda$  hyperons covers the range  $0.4 \lesssim p_T \lesssim 4$  GeV/ $c$  and  $-1.5 \lesssim y \lesssim 1.0$  but the detection efficiency strongly depends on azimuthal angle,  $p_T$  and  $y$ . Thus we have to introduce differential corrections to avoid biases when averaging  $v_2$  over rapidity and transverse momentum. Multiplicative factors were introduced for every  $\Lambda$  particle to correct the  $\Lambda$  yields for detector and reconstruction efficiency. They were determined as ratios of published  $\Lambda$  yields [15], parametrized by the Blast Wave model, to the measured raw  $\Lambda$  yields.

The elliptic flow analysis is based on the standard procedure outlined in [8, 16] to reconstruct the event plane for each event and the corrections for the event plane resolution. The event plane is an experimental estimator of the true reaction plane and is calculated from the azimuthal distribution of primary charged  $\pi$  mesons. Identification of pions is based on  $dE/dx$  measurements in the TPCs. To avoid possible auto-correlations, tracks associated with  $\Lambda$  candidates are excluded from the event plane calculation. The method to determine the event plane azimuthal angle  $\Phi_{2EP}$  uses the elliptic flow of pions, according to the formula:

$$\begin{aligned} X_2 &= \sum_{i=1}^N p_T^i [\cos(2\phi^i) - \langle \cos(2\phi) \rangle], \\ Y_2 &= \sum_{i=1}^N p_T^i [\sin(2\phi^i) - \langle \sin(2\phi) \rangle], \\ \Phi_{2EP} &= \frac{1}{2} \tan^{-1} \left( \frac{Y_2}{X_2} \right), \end{aligned} \quad (1)$$

where  $X_2, Y_2$  are the components of the event plane flow vector  $\mathbf{Q}_2$  and the sums run over accepted charged pion tracks in an event. The acceptance correction is based on the recentering method [8] which consists of subtracting in Eq. 1 the mean values  $\langle \cos(2\phi) \rangle$  and  $\langle \sin(2\phi) \rangle$ . These mean values are calculated in bins of  $p_T$  and rapidity for all pions in those events which contain at least one  $\Lambda$  hyperon candidate. The values were stored in a 3-dimensional matrix of 20  $p_T$  intervals, 50 rapidity intervals, and eight centrality bins. A second level acceptance correction is done by using mixed events. We used

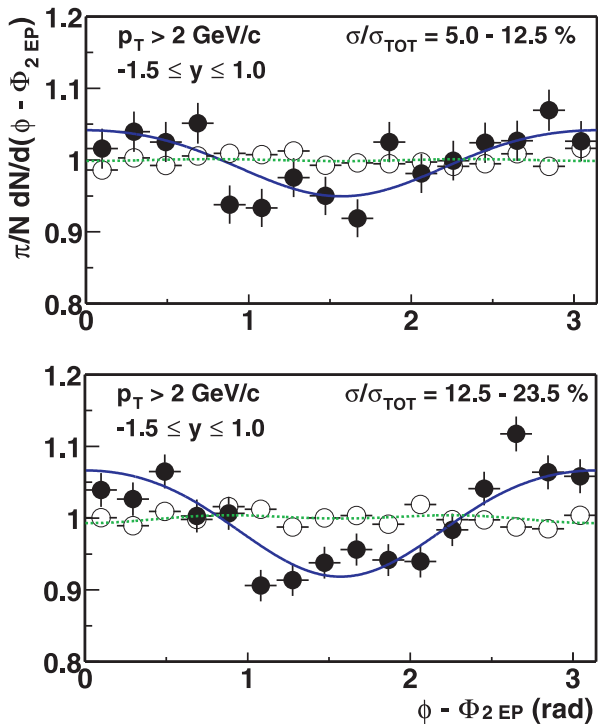


FIG. 1: (color online). Azimuthal distributions of  $\Lambda$  hyperons with respect to the event plane for real events (solid symbols) and mixed-events (open symbols) in two centrality bins. The curves are Fourier expansion fits (see text Eq. (2)).

10 mixed events for each real event. Particles for mixed events are randomly selected from different events in the same centrality bin with at least one  $\Lambda$  hyperon. The final angular distributions are obtained by dividing the real  $\Lambda$  angular distribution by the mixed event distribution to remove the acceptance correlations remaining after re-centering. The corrected  $\Lambda$  azimuthal distributions are then fitted with a truncated Fourier series:

$$\frac{dN}{d(\phi - \Phi_{2EP})} = \text{const} \times (1 + v_2^{obs} \cos[2(\phi - \Phi_{2EP})] + v_4^{obs} \cos[4(\phi - \Phi_{2EP})]). \quad (2)$$

The elliptic flow  $v_2$  is evaluated by dividing the observed anisotropy  $v_2^{obs}$  by the event plane resolution  $R$ :

$$v_2 = \frac{v_2^{obs}}{R}. \quad (3)$$

The resolution,

$$R = \sqrt{2\langle \cos[2(\Phi_{2EP}^a - \Phi_{2EP}^b)] \rangle},$$

is calculated from the correlation of two planes  $(\Phi_{2EP}^a, \Phi_{2EP}^b)$  for random sub-events with equal multiplicity. The results are  $R = 0.27, 0.34$  and  $0.40$  for centrality

bins 1, 2 and 3, respectively. The total errors in Figs. 2-4 are given by the quadratic sum of contributions from the statistical error of the signal, the uncertainty due to the background subtraction, the mixed event correction and event plane resolution. The observed hexadecupole anisotropy  $v_4^{obs}$  is consistent with zero within statistical errors for all centrality bins.

### III. RESULTS

The final statistics in our sample consists of about  $10^6$   $\Lambda$  candidates. This allows flow analysis for several rapidity and  $p_T$  bins. Two sample azimuthal distributions of  $\Lambda$

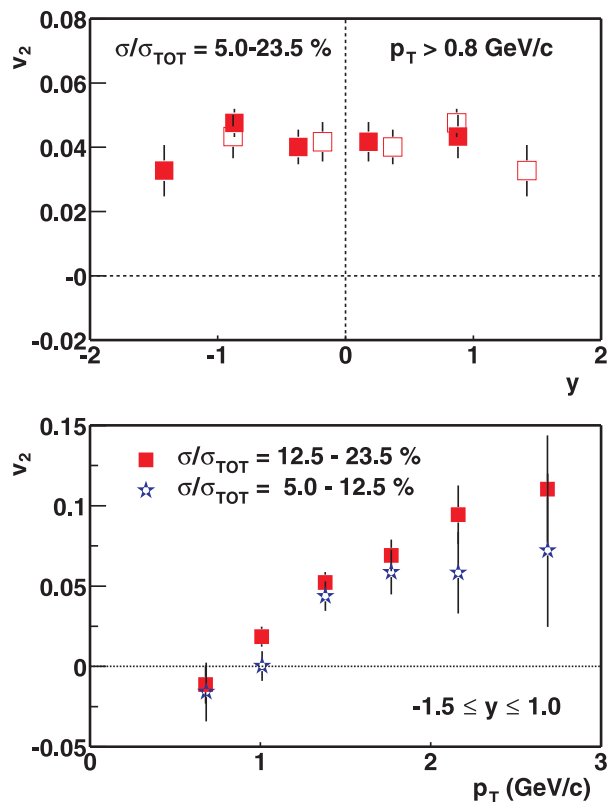


FIG. 2: (color online). Elliptic flow of  $\Lambda$  hyperons as a function of rapidity (top) and  $p_T$  (bottom). The open points in the top graph have been reflected about midrapidity.

hyperons with respect to the estimated reaction plane for real and mixed events are shown in Fig. 1. The curves represent results of fits with the truncated Fourier series Eq. (2). The distributions exhibit a strong correlation for real events (full symbols and curves). As expected, no correlation is observed for mixed-events (open symbols, dashed curves). The  $p_T$  averaged elliptic flow is obtained from all identified  $\Lambda$  hyperons without  $p_T$  cuts. It exhibits no significant dependence on rapidity as shown in Fig. 2(top). The absence of a rapidity dependence of  $v_2(y)$  was also observed for protons (see Fig. 6 in Ref. [8]) in mid-central events. We use the  $\Lambda$  sample

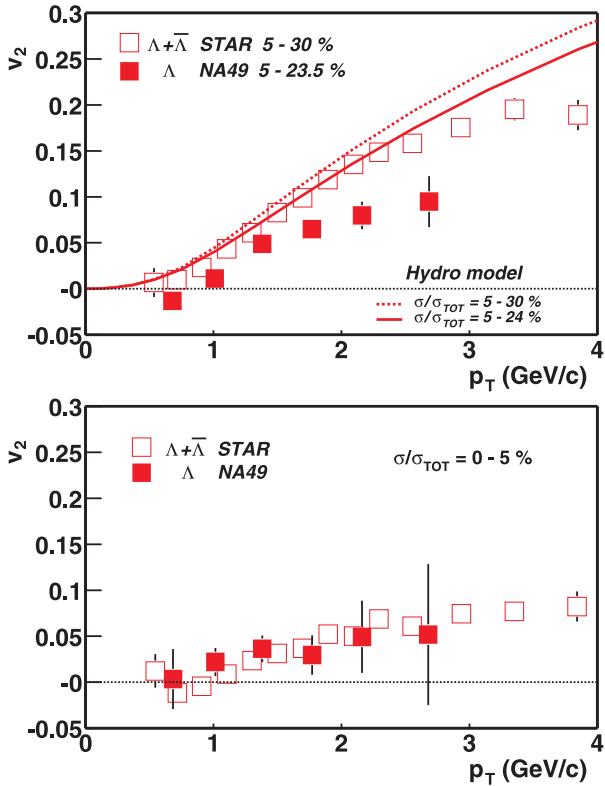


FIG. 3: (color online). Elliptic flow of  $\Lambda$  hyperons as a function of  $p_T$  from mid-central (top) and central (bottom) events measured by the STAR (open symbols) and NA49 (solid symbols) experiments. Curves are hydrodynamical model predictions at RHIC energy for the two different centrality bins.

from the full rapidity range of the data in Fig. 2(top) for the study of  $v_2$  as a function of  $p_T$ . The  $p_T$  dependence of rapidity-averaged  $\Lambda$  elliptic flow is shown in the bottom plot of Fig. 2 for two centrality ranges. The  $v_2$  parameter significantly increases with transverse momentum, the rise being stronger for more peripheral events. Fig. 3 shows a comparison of  $v_2(p_T)$  of  $\Lambda$  hyperons for mid-central and central (0-5%) events measured by the NA49 and STAR experiments [17]. The NA45 collaboration recently also presented preliminary results in Pb+Au collisions at the top SPS energy [18] which agree well with the NA49 results (not shown). For mid-central collisions at SPS energy the elliptic flow grows linearly with  $p_T$  up to  $\sim 2$  GeV/c, but the increase is steeper at RHIC than at SPS energy. It should be noted that RHIC mid-central data have been measured in the centrality range  $\sigma/\sigma_{TOT} = 5-30\%$  while SPS events are somewhat more central. The effect of different centrality ranges has been estimated by hydrodynamic calculations [19, 20] at RHIC energy for the slightly different centrality bins of NA49 and STAR. As shown by the corresponding curves in Fig. 3 this explains only partially the difference between both measurements. For central collisions NA49 and STAR results do not differ signifi-

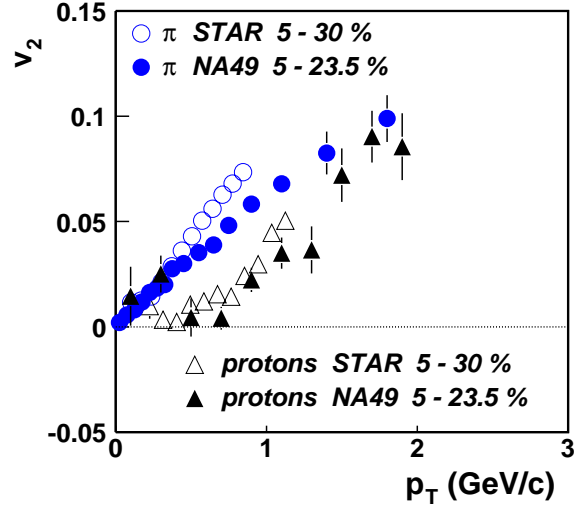


FIG. 4: (color online). Elliptic flow for charged pions (circles) and protons (triangles) as a function of  $p_T$  from mid-central events measured by the STAR [9] (open symbols) and NA49 [8] (solid symbols) experiments.

cantly (Fig. 3 bottom). A comparison of  $v_2$  of pions and protons obtained by NA49 [8] and STAR [9] for mid-central collisions is shown in Fig. 4. The NA49 values were obtained as the cross section weighted averages of the measurements published in [8] for the appropriate centrality range. As observed for  $\Lambda$  hyperons,  $v_2$  of pions also rises faster with  $p_T$  at RHIC than at SPS. Protons seem to exhibit a similar trend, but the limited  $p_T$  range and the larger measurement errors do not allow a firm conclusion.

A comparison of  $v_2(p_T)$  for pions, protons and  $\Lambda$  hyperons as measured by the NA49 experiment in mid-central events is displayed in Fig. 5. The elliptic flow grows linearly with  $p_T$  for all particle species but the rise for pions starts from  $p_T$  close to zero while for protons and  $\Lambda$  particles it starts from  $p_T \approx 0.5$  GeV/c. The elliptic flow for pions is significantly larger than that for heavier particles although at  $p_T \approx 2$  GeV/c the flow becomes similar for all particle species. Data are reproduced by blast wave fits [5, 21] (dashed curves in Fig. 5) with the following parameters: freeze-out temperature  $T = 92$  MeV, mean transverse expansion rapidity of the shell  $\rho_0 = 0.82$ , its second harmonic azimuthal modulation amplitude  $\rho_a = 0.021$ , and a spatial eccentricity parameter  $s_2 = 0.033$ . The values of freeze-out temperature and expansion rapidity are consistent with those obtained from  $m_T$  spectra and Bose-Einstein correlations [22]. In Fig. 5 the measured values of  $v_2$  are also compared to hydrodynamical model calculations [23] assuming a first-order phase transition to a QGP at the critical temperature  $T_c = 165$  MeV. The initial condi-

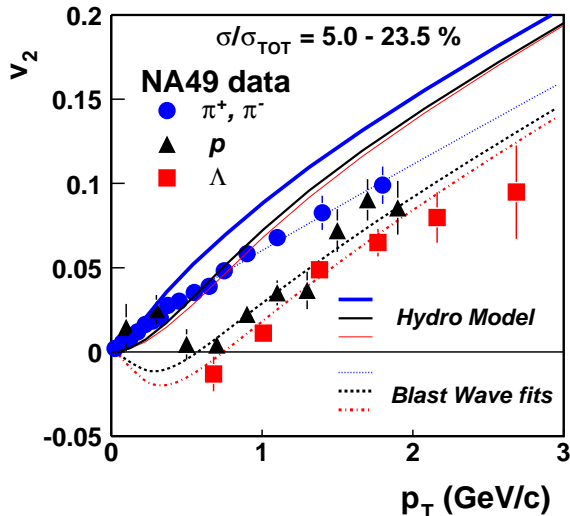


FIG. 5: (color online). Elliptic flow for charged pions (circles), protons (triangles) and  $\Lambda$  hyperons (squares) as a function of  $p_T$  from 158A GeV Pb+Pb mid-central events measured by the NA49 experiment. Curves are blast wave fits and hydrodynamic model predictions for  $\sqrt{s_{NN}} = 17.2$  GeV.

tions employed for the hydrodynamical calculations at SPS are: initial energy density  $\epsilon_0 = 9.0$  GeV/fm<sup>3</sup>, baryon density  $n_b = 1.1$  fm<sup>-3</sup>, thermalization time  $\tau_0 = 0.8$  fm/c. The initial conditions were fixed as in [24] by requiring a good fit to the  $p_T$  spectra of protons and negatively charged particles in central Pb+Pb collisions at the SPS. With the freeze-out temperature  $T_f = 120$  MeV tuned to reproduce particle spectra, the model calculations significantly overestimate the SPS results for semi-central collisions (full curves in Fig. 5) in contrast to predictions at RHIC energy which agree quite well with data for  $p_T \lesssim 2$  GeV/c [17] (see Fig.3). The discrepancy at SPS may indicate a lack of complete thermalisation or a viscosity effect. However, the model reproduces qualitatively the characteristic hadron-mass ordering of elliptic flow. Thus the data support the hypothesis of early development of collectivity. On the other hand, the magnitude and trends of elliptic flow, measured by the second Fourier coefficient  $v_2$  is found to be underpredicted by a hadronic cascade model [25]. A more comprehensive description of experimental results was found by coupling a hadronic rescattering phase to the hydrodynamical evolution and hadronisation [4]. This model can reproduce  $m_T$  spectra and elliptic flow both at top SPS energy and RHIC consistently, although predictions of  $v_2$  for exactly the centrality range of the present analysis are not published in the literature. One should note, however, that none of the hydrodynamical models have yet been able to describe Bose-Einstein correlations successfully.

Quark coalescence models [12] have been used to ex-

plain the quark number scaling observed at RHIC for  $v_2$  in the intermediate  $p_T$  region. Fig. 6 shows the scal-

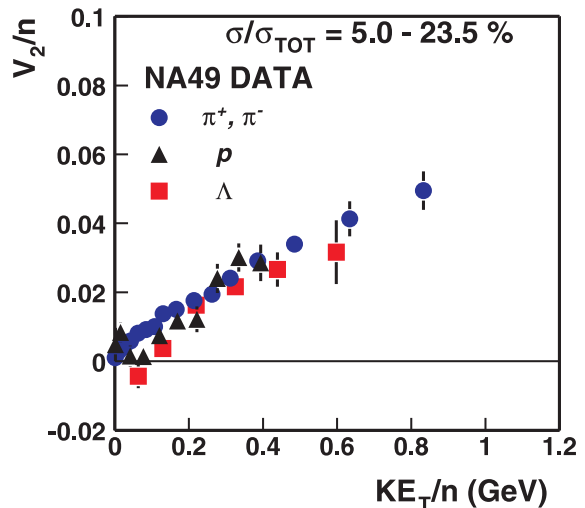
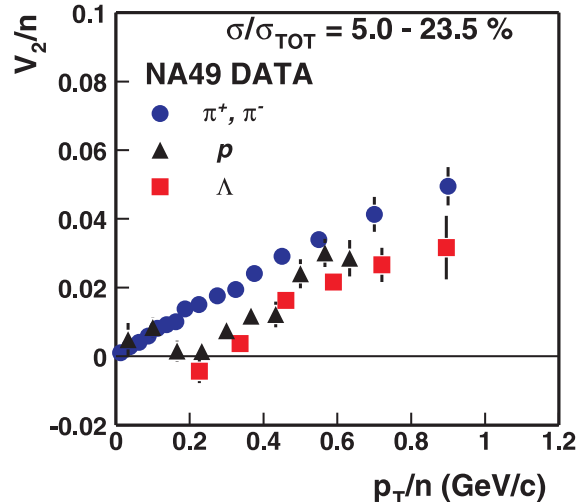


FIG. 6: (color online). Elliptic flow for charged pions (circles), protons (triangles) and  $\Lambda$  hyperons (squares) scaled by the number of constituent quarks  $v_2/n$  as a function of  $p_T/n$  (top) and  $KE_T/n$  (bottom) from 158A GeV Pb+Pb mid-central events measured by the NA49 experiment.

ing behavior of the  $v_2$  measurements of NA49 at the SPS. The values of  $v_2$  shown in Fig. 5 were divided by the number of constituent quarks  $n = 3$  for baryons and  $n = 2$  for mesons.

When plotting  $v_2/n$  versus  $p_T/n$  approximate scaling was observed at RHIC [9, 11] except for pions. The NA49 measurements (Fig. 6, top) are consistent with this result in the  $p_T$  range covered by the data. The deviation of the pions from the universal curve has been attributed to the Goldstone nature of the pion (its mass is smaller than the sum of masses of its constituent quarks) or to the effect of resonance decays [26].

The variable  $KE_T = m_T - m$ , where  $m_T$  is the transverse mass and  $m$  the rest mass of the particle, was proposed in [27] as an alternative to  $p_T$  since pressure gradients which give rise to azimuthal asymmetry may naturally lead to collective transverse energy of produced particles. Good scaling for all particle species is seen when  $v_2/n$  is plotted versus  $KE_T/n$  in the range  $KE_T/n \lesssim 0.8$  GeV covered by the SPS data (Fig. 6, bottom). This behaviour was first observed at RHIC and interpreted as a result of hydrodynamic evolution [27]. The data of NA49 do not reach higher transverse momenta at which a decisive test of coalescence models would be possible.

#### IV. SUMMARY

In summary, we report the first measurement of the anisotropic flow parameter  $v_2$  for  $\Lambda$  particles from Pb+Pb collisions at  $\sqrt{s_{NN}} = 17.2$  GeV. Elliptic flow of  $\Lambda$  hyperons exhibits no significant dependence on rapidity for  $-1.5 \lesssim y \lesssim 1.0$ . It rises linearly with  $p_T$  and is smaller than  $v_2$  for pions. Both features are quantitatively reproduced by the Blast Wave parametrization but only qualitatively by the hydrodynamic model. The increase of  $v_2$  with  $p_T$  is weaker at SPS than at RHIC energy. The observation of significant elliptic flow and its mass depen-

dence suggest strong collective behaviour of the matter produced in collisions of heavy nuclei already at the SPS. Hydrodynamic models with a deconfinement phase transition and a microscopic freezeout treatment appear to provide a consistent description of  $v_2$  and  $m_T$  spectra at both top SPS and RHIC energies [4]. Quark number scaling of elliptic flow ( $v_2/n$  versus  $KE_T/n$ ) was shown to hold also at the SPS. However, the limited  $p_T$  reach of the data does not allow a decisive test of the quark coalescence hypothesis.

#### Acknowledgments

This work was supported by the US Department of Energy Grant DE-FG03-97ER41020/A000, the Bundesministerium für Bildung und Forschung Grant 06F-137, Germany, the Virtual Institute VI-146 of Helmholtz Gemeinschaft, Germany, the Polish State Committee for Scientific Research (1 P03B 006 30, 1 P03B 097 29, 1 P03B 121 29, 1 P03B 127 30), the Hungarian Scientific Research Foundation (T032648, T032293, T043514), the Hungarian National Science Foundation, OTKA, (F034707), the Polish-German Foundation, the Korea Science & Engineering Foundation (R01-2005-000-10334-0) and the Bulgarian National Science Fund (Ph-09/05).

- 
- [1] J. Y. Ollitrault, Nucl. Phys. A **638**, 195 (1998).  
 [2] P. F. Kolb, J. Sollfrank and U. W. Heinz, Phys. Rev. C **62**, 054909 (2000).  
 [3] J. Y. Ollitrault, Phys. Rev. D **46**, 229 (1992); H. Sorge, Phys. Rev. Lett. **82**, 2048 (1999).  
 [4] D. Teaney, J. Lauret and E. V. Shuryak, Phys. Rev. Lett. **86**, 4783 (2001) and nucl-th/01110037.  
 [5] P. Huovinen, P. F. Kolb, U. W. Heinz, P. V. Ruuskanen and S. A. Voloshin, Phys. Lett. B **503**, 58 (2001).  
 [6] R. Snellings [STAR Collaboration], Heavy Ion Phys. **21**, 237 (2004)  
 [7] N. Bastid *et al.* [FOPI Collaboration], Nucl. Phys. A **622**, 573 (1997); A. Andronic *et al.* [FOPI Collaboration], Nucl. Phys. A **679**, 765 (2001); J. Barrette *et al.* [E877 Collaboration], Phys. Rev. C **55**, 1420 (1997); H. Appelshauser *et al.* [NA49 Collaboration], Phys. Rev. Lett. **80**, 4136 (1998).  
 [8] C. Alt *et al.* [NA49 Collaboration], Phys. Rev. C **68**, 034903 (2003).  
 [9] J. Adams *et al.* [STAR Collaboration], Phys. Rev. C **72**, 014904 (2005)  
 [10] J. Adams *et al.* [STAR Collaboration], Phys. Rev. Lett. **95**, 122301 (2005).  
 [11] S. S. Adler *et al.* [PHENIX Collaboration], Phys. Rev. Lett. **91**, 182301 (2003)  
 [12] V. Greco, C.M. Ko and P. Levai, Phys. Rev. C **68**, 034904 (2003); V. Greco, C.M. Ko and P. Levai, Phys. Rev. Lett. **90**, 202302 (2003); D. Molnar and S.A. Voloshin, Phys. Rev. Lett. **91**, 092301 (2003).  
 [13] S. V. Afanasiev *et al.* [NA49 Collaboration], Nucl. Intr. Meth. A **430**, 210 (1999).  
 [14] H. Appelshauser *et al.* [NA49 Collaboration], J. Phys. G **25**, 469 (1999); L.S. Barnby, Ph.D. Thesis, University of Birmingham (1999).  
 [15] T. Anticic *et al.* [NA49 Collaboration], Phys. Rev. Lett. **93**, 022302 (2004)  
 [16] S. A. Voloshin and A. M. Poskanzer, Phys. Lett. B **474**, 27 (2000).  
 [17] J. Adams *et al.* [STAR Collaboration], Phys. Rev. Lett. **92**, 052302 (2004).  
 [18] J. Milosević *et al.* [NA45 Collaboration], Nucl. Phys. A **774**, 503 (2006).  
 [19] P. Huovinen, Nucl. Phys. A **761**, 296 (2005), and private communication.  
 [20] The initial conditions employed for the hydrodynamical calculations at RHIC are:  $\epsilon_0 = 23$  GeV/fm<sup>3</sup>,  $n_b = 0.12$  fm<sup>-3</sup>,  $\tau_0 = 0.6$  fm/c .  
 [21] C. Adler *et al.* [STAR Collaboration], Phys. Rev. Lett. **87**, 182301 (2001).  
 [22] S. Kniese *et al.* [NA49 Collaboration], nucl-ex/0601024 (2006).  
 [23] P. Huovinen, private communication (2005),  $T_c = 165$  MeV,  $T_f = 120$  MeV,  $EoS=Q$ .  
 [24] P. F. Kolb, J. Sollfrank and U. W. Heinz, Phys. Lett. B **459**, 667 (1999); P. F. Kolb, J. Sollfrank, P. V. Ruuskanen and U. W. Heinz, Nucl. Phys. A **661**, 349 (1999); P. F. Kolb, P. Huovinen, U. W. Heinz and H. Heiselberg, Phys. Lett. B **500**, 232 (2001).  
 [25] M. Bleicher and H. Stoecker, Phys. Lett. B **526**, 309 (2002).

- [26] V. Greco and C.M. Ko, Phys. Rev. C **70**, 024901 (2004).
- [27] M. Issah and A. Taranenko [PHENIX Collaboration], nucl-ex/0604011; A. Adare *et al.* [PHENIX Collaboration], nucl-ex/0608033.